2014 ASIA-PACIFIC SOLAR RESEARCH CONFERENCE

Peer Reviewed Paper

Rhys Jacob

Techno-Economic Analysis of Phase Change Material Thermal Energy Storage Systems in High Temperature Concentrated Solar Power Plants

Rhys Jacob, Wasim Saman, Martin Belusko and Frank Bruno

Barbara Hardy Institute, University of South Australia, Mawson Lakes, SA 5095, Australia

E-mail: rhys.jacob@mymail.unisa.edu.au

Abstract

Thermal energy storage (TES) is utilised to supplement curtailed energy production that occurs in concentrated solar power (CSP) plants due to cloud cover or the setting sun. Phase change materials (PCMs) offer a potentially more economical solution than the traditional two-tank molten salt storage system. PCM thermal storage can be configured either as a coil in tank arrangement where the working fluid of the power block flows through the coil, or where the heat transfer fluid (HTF) flows through a tank of encapsulated phase change material (EPCM). This paper presents a preliminary techno-economic analysis of a variety of combinations for both configurations. The thermal performance of a coil in tank system is defined by the heat exchange area of the coil by which the working fluid can exchange heat with the PCM. For the EPCM system the thermal performance is defined by total surface area of the capsules which can exchange heat with the HTF. In this study the working fluid considered is sCO_2 and the HTF is a eutectic molten salt. From previous research, it is possible to estimate the useful extracted energy from each storage system. Various PCMs were investigated including inorganic materials, molten salts and alloys for both systems. For the coil-in-tank configuration the coil material were SS316, Incolloy and Titanium. An EPCM system investigated the use of SS304L, copper and silicon carbide as an encapsulation (also known as the shell) material.

Nomenclature

Q	volumetric energy density, J/m3	**c**	coating thickness of capsule, m
Cp	specific heat capacity, J/kgK	**v**	capsule void
T	temperature, °C	**ρ**	density, kg/m3
ΔH	latent heat of fusion, J/kg	**ε**	Porosity
V	volume, m^3	**PCM**	phase change material
h	height, m	**C**	charging temperature
r	radius, m	**D**	discharging temperature
C	cost, $	**HTF**	heat transfer fluid
C*	cost factor, $/kg	**T**	Tank
C**	cost factor, $/$m^2$	**S**	stored energy
C***	cost factor, $/each	**E**	Encapsulate
$C^{\#}$	cost factor, $/kWh	**ss**	stainless steel
$C^{\#\#}$	cost factor, $/hr	**F**	Foundation
$C^{\#\#\#}$	cost factor	**I**	Insulation
m	mass, kg	**cap**	Capsule
C	preliminary cost, $	**SM**	storage material
C	total cost, $	**L**	Labour
R	total cost, $/kWh	**s**	Shell
w	wall thickness, m	**FB**	fluidised bed
S	stored energy, J	**PC**	preformed capsule
SA	surface area of capsule, m^2	**f**	filling
#	Number	**EP**	electroplate

1. Introduction

With the increasing need to use renewable energy to avoid irreversible climate damage, both the technology and economics of renewable energy supply methods need to be explored. A promising candidate for large scale renewable energy production is concentrated solar power (CSP). However the major drawback of using such a system remains the inability to supply continuous energy to match the demand profile. Energy production is curtailed or completely stalled during periods of limited or no sunlight. A workable solution to this problem is thermal energy storage (TES). TES utilises the ability of materials to store excess energy as heat during low demand times. This energy can then be accessed as demand increases. Currently there are many ways to achieve TES with CSP. One of the more promising and cost effective ways remains latent heat storage. When heat is applied to the system (charging), the material (also known as a phase change material (PCM)) stores energy as it is heated. As the PCM approaches its phase change temperature, it can continue to store this energy at a nearly constant temperature. This leads to a much larger energy density than that of sensible heat storage. When the heat is removed from this material (discharging) the energy stored in the material is released. The chief concern with this type of storage remains the low thermal conductivity of most PCMs. A low thermal conductivity restricts the efficient transfer of heat from the heat transfer fluid (HTF) to the PCM, which leads to long charge and discharge times. This scenario is undesirable for efficient power generation. A convenient method of applying PCMs in a coil in tank arrangement, in which the HTF flows through a coil surrounded by PCMs (Tay et al, 2012). This configuration has the advantage of enabling the HTF to be the working fluid of the power block, eliminating the cost of heat tracing systems and a molten salt pump. However, a costing analysis of the PCM/coil configuration has yet to be undertaken which considers appropriate materials. Research has shown that the most effective approach involves using multiple PCMs, and therefore a variety of PCMs with different melting points are considered Liu et al (2014).

An additional effective method to overcome the thermal resistance within latent heat thermal storage systems (LHTSS), is through encapsulated PCM. The encapsulation of the PCM increases the contact surface area. It also helps to control volume changes in the system and increases the compatibility of the PCM with the construction materials. This study is a techno-economic analysis of three (3) potential encapsulated phase change material (EPCM) designs. This work is meant to build on the knowledge gained from previous studies (Nithyanandam and Pitchumani, 2014; Mathur et al, 2013) to ensure the most cost effective EPCM design can be established. The distinguishing features of this analysis over previous studies is the investigation into the effect of the shell on the system (both on the total volume and the sensible heat) and the ability to compare the costs of various encapsulating methods.

2. Methodology

The EPCM storage systems designed in this analysis are required to store 29MWh of energy when fully charged. Each of the investigated cases differ slightly with regards to shell material, method of encapsulation, the HTF used and the PCM to be encapsulated. Where possible, combinations of HTF/shell material, PCM/shell material and shell material/method of encapsulation were chosen to be compatible. The design considerations used in each case can be found in Table 1.

Table 1-Investigated case design considerations

Parameter	**Case 1**	**Case 2**	**Case 3**
	Material		
Shell	Silicon Carbide	Copper	Stainless Steel (304L)
HTF	Molten Salt	Low pressure CO_2 (1atm,600°C)	Low pressure CO_2 (1atm,600°C)
PCM	Al-Si_{12}	Al-Si_{12}	$Ca(NO_3)_2$
Method of Encapsulation	Fluidised bed	Electroplating	Preformed

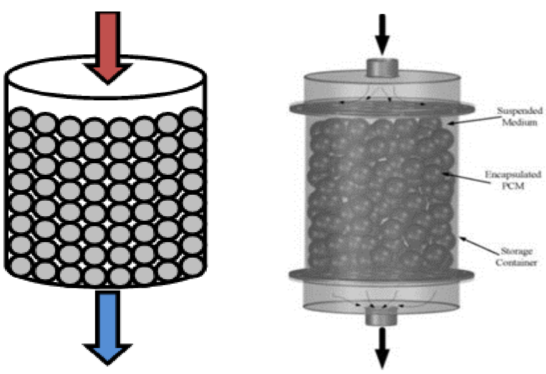

Figure 1-EPCM system

Silicon carbide was chosen as a shell material because of its good thermal conductivity, good thermal stability and its predicted compatibility with molten salt HTFs. Copper was investigated as a shell material because of its high thermal conductivity while stainless steel was chosen because of its ease of manufacture and low corrosivity. The overall design of the system will be the same for each investigated case. Each will consist of a single thermocline tank in which the hot HTF fluid will flow in direct contact with the EPCMs. The cold HTF will then flow back to the solar field to be recharged. The HTF in each case is assumed to enter at 600˚C and leave at 200˚C. The configuration of the proposed system is shown in Figure 1. A single thermocline tank was chosen for its low cost, ease of fabrication and ease of use. Spherical capsules were chosen due to their enhanced heat transfer rates and ease of manufacture. In this particular analysis the use of multiple PCMs (a cascaded system) has not been investigated. To compare each system, each case was subject to certain constraints. These constraints are shown in Table 2. Each constraint was chosen as being reasonable for the proposed systems.

Values for the physical and thermophysical data for the HTF, PCM and shell material was sourced from relevant literature (Kenisarin, 2010; Jonemann, 2013; Lee Kee Group; Ceramic Industry; Engineers Edge; Peace Software) and is shown in Table 3. Each capsule is to be spherical with the parameters outlined in Table 4. The cost data that has been used in this analysis has been sourced from relevant literature (Nithyanandam and Pitchumani, 2014; Mathur et al, 2013; Kelly and Kearney, 2006; Herrmann et al, 2004; Mazzilli and Lenau; Infomine 2014) and potential suppliers (GY Steel Ball co, 2014; Tianjin Taixin Weiye Metallic Materials Co., Ltd, 2014; MEPS, 2014) and is shown in Table 5.

Table 2-System constraints

Parameter	**Value**
Void Fraction [ε]	0.37
Charging Temperature [T_C] (°C)	200
Discharging Temperature [T_D] (°C)	600
Energy Stored [S] (J)	1.04E+11
Tank radius [r_t] (m)	2

Table 3-Physical data for case 1, 2 and 3

Parameter	**Case 1**	**Case 2**	**Case 3**
Density of PCM [ρ_{PCM}] *(kg/m³)*	2540	2540	2113
Heat Capacity of PCM [Cp_{PCM}] *(J/kgK)*	963	963	910
PCM melting temperature [TM] (°C)	557	557	560
Enthalpy of PCM [ΔH] (J/kg)	498000	498000	145000
Density of HTF [ρ_{HTF}] *(kg/m3)*	2150	0.61	0.61
Heat Capacity of HTF [Cp_{HTF}] *(J/kgK)*	800	1196	1196
Heat capacity of shell [Cp_s] *(J/kgK)*	628	386	500
Density of shell [ρ_s] *(kg/m3)*	3210	8960	7900

Table 4-Capsule parameters

Parameter	**Value**
Capsule radius inner [r_{cap}] (m)	0.004
Capsule thickness [c] (m)	0.0002
Capsule void [v]	0.85
Capsule surface area [SA] (m2)	2.01E-04
Capsule volume [V] (m3)	2.68E-07

Table 5-Cost data for case 1, 2 and 3

Cost	**Case 1**	**Case 2**	**Case 3**
Cost of PCM [C*p] *($/kg)*	2	2	0.23
Cost of shell [C*s] *($/kg)*	1.35	6.9	2.5
Cost of HTF [C^*_{HTF}] *($/kg)*	1.4	0.01	0.01

A sensitivity analysis was also performed on key parameters such as material cost (PCM, HTF and stainless steel) and encapsulation cost. The material cost in particular is a parameter that can vary significantly. The difficulty in obtaining accurate information on material data, material costs and manufacturing costs have left the economic analysis with an estimated accuracy of 30%. The conflict of values (or lack of values) from literature and suppliers has been determined as warranting further investigation. Figure 2 presents the coil-in-tank arrangement. The coil can be designed to accommodate SCO2 at 20 MPa and 550°C, and therefore must have high strength, and compatible with the PCM. The PCMs being considered include chloride salts, carbonate salts and aluminium alloys as presented in Table 8. To overcome corrosion issues, the tubing should be made from Incolloy, 316 stainless steel and titanium for each PCM, respectively.

The material costings provided in Table 8 are based on bulk prices of the raw material. Determining the amount of tubing required was based on CFD modelling and using the effectiveness-NTU method as explained in Liu et al (2014). From this value the combined cost of each configuration could be found. A fixed temperature rise for the sensible component of storage of 300°C, was applied to all PCMs to enable a direct comparison of each arrangement.

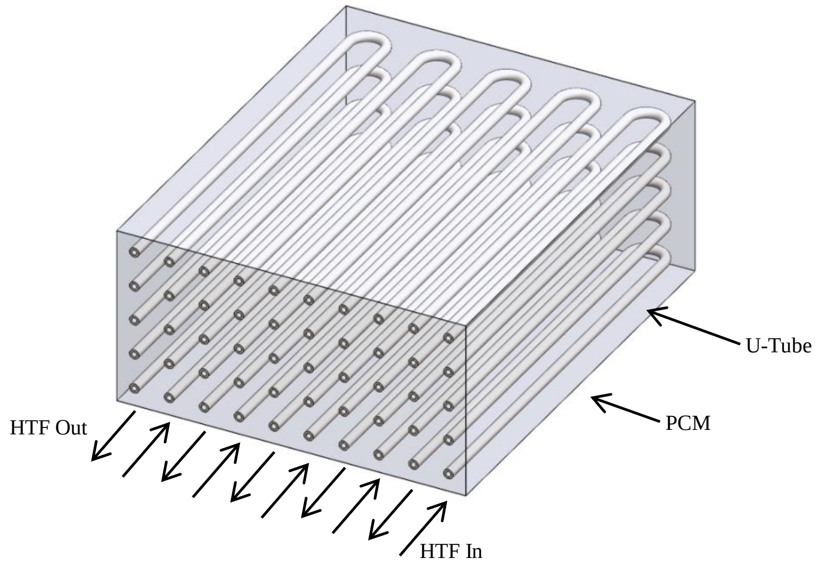

Fig. 2. Tube-in-tank (shell and tube) PCM energy storage system with U-Tube.

2.1 Tank design and costing

The cost of the tank for each encapsulated PCM system was found using Equation 1. Tank costs were not investigated for the coil – in –tank arrangement.

This equation is based on previous work by Nithyanandam and Pitchumani (2014) with an additional factor added for indirect costs such as labour and installation. At this stage tank costs were not considered for the coil – in –tank arrangement.

$$C_t = ([\rho_{ss} h(\pi(r_t + w)^2 - \pi r^2)] \times C^*{}_t + \pi r_t{}^2 C^{**}{}_F + 2\pi r_t h C^{**}{}_I) \times C^{\#\#\#}{}_l \qquad [1]$$

The density of stainless steel was assumed to be 7900kg/m3 with a cost of $3.01/kg (MEPS, 2014). The wall thickness of the tank was taken to be 0.038m while the cost of the insulation and the foundation was $235/m2 and $1210/m2 respectively (Kelly and Kearney, 2006; Herrmann et al, 2004). $C^{\#\#\#}{}_l$ is the cost of constructing new equipment and was assumed to be 1.25 (Worley Parsons, 2012). The height of the tank (Equation 4) was calculated from the volume of the tank required (Equation 3) which in turn is based on the energy density of the storage material (Equation 2).

$$Q_t = ([\rho_{PCM} \times Cp_{PCM} \times (1-\varepsilon) \times (T_C - T_D)] + [\rho_{PCM} \times \Delta H \times (1-\varepsilon)]) + (\rho_{HTF} \times Cp_{HTF} \times \varepsilon \times (T_C - T_D)) + (Cp_s \times \rho_s \times (T_C - T_D)) \qquad [2]$$

$$V_t = {}^{S}\!/_{Q_t} \qquad [3] \qquad\qquad h = {}^{V_t}\!/_{\pi r_t{}^2} \qquad [4]$$

2.2 Storage material cost

The cost of the storage material is simply the cost of the raw materials. The total cost of the storage materials can be found from Equation 5. For the coil in tank arrangement the material cost is related to the raw material cost of the PCM and the coil material.

Based on CFD modelling the amount of coil material was determined which enables 80% of the energy stored to be discharged, (discharged at maximum rated power output).

$C_{SM} = \pi r_t^2 h\left((\rho_{PCM}(1-\varepsilon)C^*_p) + (\rho_{HTF}\varepsilon C^*_{HTF})\right)$ [5]

2.3 Fabrication Costs

For each investigated case the method of encapsulation is different, which results in very different encapsulation costs. For the coil in tank arrangement fabrication costs are expected to be a small component and similar across all options, and therefore ignored in this study.

2.3.1 Fluidised bed

The cost of the fluidised bed process is based on previous work by Nithyanandam and Pitchumani (2014) and is given by Equation 6 and 7.

$C^*_{E,FB} = (\frac{r_{cap}}{0.005})^{0.3} \times C^*_{E0}$ [6] $C_{E,FB} = C^*_{E,FB} \times m_{PCM}$ [7]

Where the mass of the PCM required is given by Equation 8.

$m_{PCM} = (1-\varepsilon) \times V_t \times \rho_{PCM}$ [8]

The cost of encapsulating 1kg of PCM in this method is based on previous work by Nithyanandam and Pitchumani (2014) and Mathur et al (2013), where the cost of encapsulating 1kg of PCM in a capsule with radius 0.005m is \$0.75/kg (C^*_{E0}) (Nithyanandam and Pitchumani, 2014; Mathur et al, 2013).

2.3.2 Electroplating

The cost of electroplating the PCM involves the cost of the electroplater and the cost of the shell material required to coat the capsule. For this scenario it is assumed the PCM can be directly electroplated and requires no pre-treatment. Equations 9, 10 and 11 can be used to calculate the electroplating cost.

$C_{E,EP} = (C_s \times \#_{cap}) + C_{EP} \times (\frac{C^{\#\#}}{60})$ [9] $C_{EP} = \left(\frac{SA \times c_S \times \rho_S \times 15000}{I_S \times E_S \times Y_S}\right) + (0.005 \times \#_{cap})$ [10]

$C_s = V_s \times \rho_s \times C^*_s$ [11]

The cost of the electroplater was taken as \$28.65/hr while the electroplating parameters (I_S, E_S and Y_S) are taken from [11]. For copper they are 300, 0.71 and 60 respectively.

Other shell material parameters can be found in Mazzilli and Lenau. The number of capsules that a system requires is given by Equation 12-13.

$\#_{cap} = \frac{m_{PCM}}{\rho_{PCM} \times V_s}$ [12]

$V_s = SA \times c$ [13]

2.3.3 Pre-formed Shells

The last method of encapsulation investigated was that of using pre-formed shells. The cost of using pre-formed shells involved the cost of the capsule, the cost to melt the PCM and the cost to fill the capsule. These costs are best described by Equations 14 and 15.

$C_{E,PC} = (\#_{cap} \times C^{***}_{cap} + C_{PC}) \times C^{\#\#\#}_f$ [14]

$C_{PC} = \frac{m_{PCM} \times Cp_{PCM} \times (T_m - 25) \times C^{\#}}{3600000}$ [15]

The cost of buying preformed capsules was taken to be \$0.001 each GY Steel Ball co (2014), the filling factor was estimated to be 1.1 and the cost of electricity was taken to be \$0.2/kWh.

3. Results and Discussion

Table 6 and Figure 3 present a summary of the key findings of this analysis. Case 3 has the lowest storage material cost of the investigated scenarios. This is due to the low cost of the PCM ($Ca(NO_3)_2$) and HTF (CO_2) used in the system. Case 1 has the lowest encapsulation cost of the three (3) scenarios.

The low cost of encapsulation is due to the fact that the fluidised bed process has low running costs, high encapsulation yield and is established in the encapsulation industry. Case 1 also has the lowest tank cost. This is due to the high energy density of the system.

The energy density of the system is largely dependent on the PCM and the HTF. As the PCM and HTF used in case 1 both have large energy densities compared to those used in case 2 and case 3, a smaller tank is needed for the same stored energy.

Table 6-Key results of analysis

Case	Cost of Storage Material ($)	Cost of Encapsulating PCM ($)	Cost of Tank ($)	Direct System Cost ($)	Total System Cost ($)	Total Cost/kWh ($/kWh)
1	270,042	70,259	90,691	430,993	461,163	15.90
2	236,395	1,036,419	104,281	1,377,095	1,473,492	50.81
3	47,168	474,612	200,985	722,764	773,358	26.67

Results from the sensitivity analysis are presented in Table 7 and Figure 4. Sensitivity analysis results suggest that case 1 is most affected by the PCM price.

A 10% rise in the PCM price ($2.2/kg) results in a total cost 5% higher than the reference case. Case 2 is also similarly affected but to a lesser extent. The change in PCM price has very little effect on case 3. This is due to the low cost of the PCM used in this case.

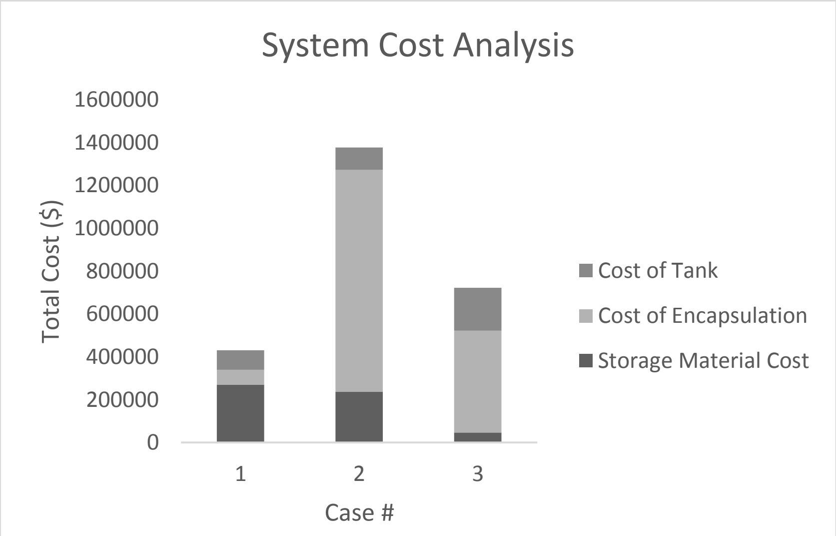

Figure 3- System Cost Analysis

It is concluded from this that the cost of the PCM starts to have a pronounced impact on the total cost of the system if the PCM cost is more than $0.8/kg. Case 1 is also the most affected by the change in the HTF cost. This is unsurprising considering the low cost of the HTF used in case's 2 and 3. The cost of the HTF has less of an impact on the total cost of the system when compared to the HTF due to the lower quantity needed. However as the cost of the HTF approaches $2/kg, there begins to be more of an effect on the total system cost. As expected the variation in stainless steel prices affects the systems with small energy densities, and therefore larger tanks, the most. Case 3 is therefore affected by the change in stainless steel price the most. Tanks that require expensive materials (such as those that require Inconel or similar materials) should be avoided where possible. For example a system which requires the tank to be constructed of Inconel will be around 40% more expensive than a system using a stainless steel tank. Systems that can use carbon steel tanks instead of stainless steel tanks are less affected, with savings of around 5%. The cost of encapsulation is a parameter that will need to be verified with future work.

For case 2 and 3 it can be seen that a small change in the cost of encapsulation can have a significant impact on the overall system cost. It is suggested that more accurate economic data on encapsulation costs be investigated more thoroughly.

Table 7-Sensitivity analysis on key parameters

Case	Total Cost/kWh ($/kWh)								
	Reference Cost	PCM Price +10%	PCM Price -10%	HTF Price +10%	HTF Price -10%	Stainless Steel Price +10%	Stainless Steel Price -10%	Cost of Encapsulation +10%	Cost of Encapsulation -10%
1	15.90	16.64	15.16	16.16	15.64	16.11	15.69	16.16	15.64
2	50.81	51.68	49.94	50.81	50.81	51.06	50.55	54.63	46.99
3	26.67	26.84	26.44	26.67	26.67	27.18	26.13	28.42	24.92

Table 8 presents a comparison of the various combinations of coil-in-tank configurations. The chloride PCMs have the lowest cost, but also the lowest energy density and require a significant amount of high cost tubing. Carbonate PCMs, have a higher energy density and the tube cost is of similar impact as the PCM cost.

Overall, any PCM with a lithium compound delivers the most expensive solution. Surprisingly the aluminium alloy is a low cost choice due to having the highest energy density and requiring a small amount of tubing. The lowest cost option involves a low cost PCM with the lowest cost tubing. However since the energy density is not as high as the alloy, if other costs such as tank and manufacturing costs were included the cost would most likely be similar.

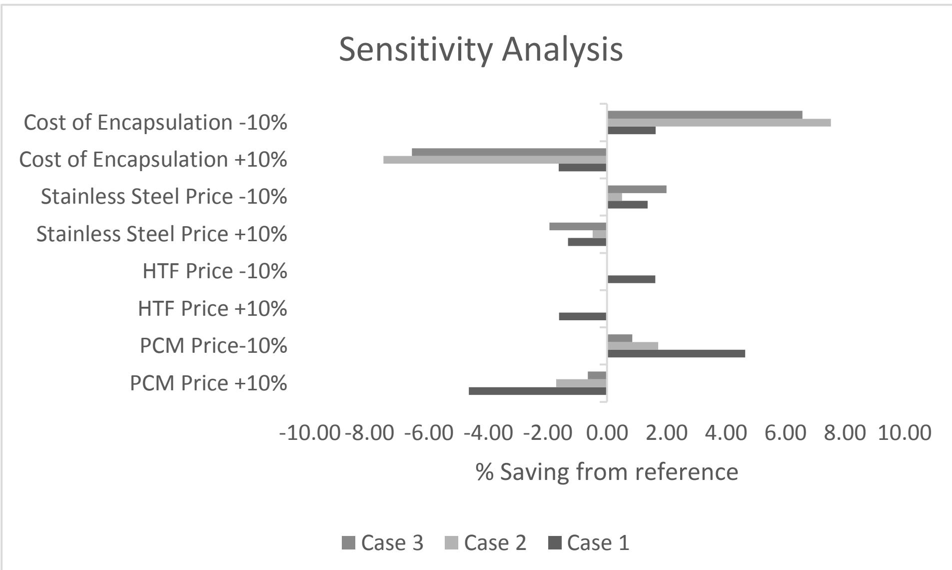

Figure 4-Sensitivity Analysis

Table 8-Coil in Tank Design Parameters

PCM WITH MELTING POINT	COIL MATERIAL	$/kWhr	kWhr/m3	Ratio of coil to PCM mass	Tube to Total Cost	PCM cost, $/kg	Tube cost, $/kg
450 PCM 40% MgCl2/60% NaCl	Incolloy 800	19.7	220	0.15	0.94	0.17	15
623 PCM 60% Na2CO3/40% NaCl	Incolloy 800	19.1	242	0.15	0.93	0.20	15
508 PCM, 35% LiCO3, 65% K2CO3	SS 316	22.9	345	0.15	0.25	3.48	6.63
560 PCM, 35% NaCl, 65% LiCl	Incolloy 800	48.3	299	0.15	0.31	5.77	15
aluminium-silicon eutectic alloy	Titanium alloy	12.1	511	0.005	0.05	2.20	25
710 PCM, 51% K2CO3, 49% Na2CO3	SS 316	10.2	315	0.15	0.61	0.74	6.63

4. Conclusions

This techno-economic analysis explored three possible EPCM designs. Each design differed in the shell material used and the method of encapsulation. Where appropriate the PCM and HTF were chosen to provide the highest energy density that could be obtained for that particular shell material. Results from this analysis suggest that the most cost effective EPCM system is the one proposed in case 1. Although this case has a higher storage material cost than the other investigated cases, the energy density is much higher. This allows a smaller tank to be used and a lower encapsulation cost to be achieved. From the sensitivity analysis it was found that the PCM cost should be below $0.8/kg to reduce the impact on the overall system. Similarly, the HTF cost should be below $2/kg. It was found there were marginal savings in the system cost when a carbon steel tank was used instead of a stainless steel tank. However tanks constructed of more expensive materials (such as Inconel etc.) should be avoided where possible. Lastly the cost of encapsulation is largely dependent on the shell material used and the method of PCM encapsulation. This is an area that has been identified as requiring more investigation to obtain more accurate economic data. As EPCMs become commercialised, this cost will significantly decrease leading to a further reduction in system costs. For coil-in-tank PCMs, the amount and cost of the tubing is a critical factor. The Analysis has identified low cost solutions; namely the aluminium alloy PCM with titanium tubing, and low cost carbonates with stainless steel coil.

References

Ceramic Industry. Material Property Charts. <https://www.ceramicindustry.com/ext/resources/pdfs/2013-CCD-Material-Charts.pdf> [Last Accessed 3 September 2014]
Engineers Edge. Thermal Conductivity of metals. <http://www.engineersedge.com/properties_of_metals.htm> [Last Accessed 29th August 2014]
GY Steel Ball co, via correspondence (2014).
Herrmann U, Kelly B, Price H. Two-tank molten salt storage for parabolic trough solar power plants. Energy (2004); 29: 883–893.
Infomine. Copper Prices. <http://www.infomine.com/investment/metal-prices/copper/> [Last Accessed 29th August 2014]
Jonemann, M. Advanced Thermal Storage System with Novel Molten Salt. National Renewable Energy Laboratory. NREL/SR-5200-58595 (2013).
Kelly B, Kearney D. Thermal storage commercial plant design for a 2-tank indirect molten salt system. National Renewable Energy Laboratory, NREL/SR-550040166, 1–32 (2006).
Kenisarin M. High-temperature phase change materials for thermal energy storage. Renewable and Sustainable Energy Reviews (2010); 14: 955‐970.
Lee Kee Group. International Standard Compositions of Aluminium Die-casting Alloys.
Liu M, Tay N.H.S, Belusko M, Bruno F. *Investigation of cascaded shell and tube latent heat storage systems for solar tower power plant*. International Conference on Concentrating Solar Power and Chemical Energy Systems, SolarPACES 2014.
Mathur A, Kasetty R, Oxley J, Mendez J, Nithyanandam K. Using encapsulated phase change salts for concentrated solar power plant. SolarPACES (2013).
Mazzilli A, Lenau A. Electroplating costs calculation. <http://polynet.dk/ingpro/surface/elecomk.htm> [Last Accessed 12th September 2014]
MEPS. World Stainless Steel Prices. < http://www.meps.co.uk/Stainless%20Prices.htm> [viewed August 2014].
Nithyanandam K, Pitchumani R. Optimization of an encapsulated phase change material thermal energy storage system. Solar Energy 107 (2014) 770–788.
Peace Software. Thermodynamic state variables of carbon dioxide. <http://www.peacesoftware.de/einigewerte/co2_e.html> [Last Accessed 12th September 2014]
Tay N.H.S, Bruno F, Belusko M. *Experimental validation of a CFD and an e-NTU model for a large tube-in-tank PCM system*. International Journal of Heat and Mass Transfer, 2012. 55: p. 5931-5940.
Tianjin Taixin Weiye Metallic Materials Co., Ltd, via correspondence (2014).
Worley Parsons. Cost of Construction New Generation Technology. Report: 101010-00676, (2012).

Acknowledgments

This research was performed as part of the Australian Solar Thermal Research Initiative (ASTRI), a project supported by the Australian Government, through the Australian Renewable Energy Agency (ARENA).